Reactivity of Biologically Important Reduced Pyridines. 2.† The Oxidation of 1-Methyl-4-phenyl-1,2,3,6-tetrahydropyridine (MPTP). An MNDO Study

Marcus E. Brewster,‡,§ James J. Kaminski,‡,⊥ and Nicholas Bodor*,‡

Contribution from the Center for Drug Design and Delivery, College of Pharmacy, University of Florida, Gainesville, Florida 32610. *Received February 5, 1988*

Abstract: In order to better understand the chemistry associated with the oxidation of 1-methyl-4-phenyl-1,2,3,6-tetrahydropyridine (MPTP), an MNDO study was performed. MPTP, the corresponding pyridinium salt (MPP^+), and eight intermediates were examined. Optimized geometries were obtained and relative stabilities determined based on charge distribution and molecular orbital (MO) structure. The occurrence of the 1-methyl-4-phenyl-2,3-dihydropyridinium ion ($MPDP^+$-2,3) in various tissue preparations, but not the corresponding 2,5-isomer ($MPDP^+$-2,5), after MPTP treatment was rationalized based on semiempirical heats of formation (ΔH_f) which showed that $MPDP^+$-2,3 was 4.7 kcal/mol more stable. In addition, charge densities generated for $MPDP^+$-2,3, $MPDP^+$-2,5, and the corresponding free base (MPDP) accurately predicted sites of nucleophilic attack as well as the mechanism of $MPDP^+$-2,3 disproportionation. The study also indicated that the one-electron reduction of MPP^+ was more difficult than the corresponding reduction of $MPDP^+$-2,3, a result consistent with experimentally determined halfwave potentials. The oxidation of the NADH model, 1-methyl-1,4-dihydronicotinamide (NMH-1,4), was then examined and comparisons were made between this transformation and MPTP oxidation. The results demonstrated the large difference in the initial ionization and suggested that reduction of the pyridinium salt (NMN^+) was more exergonic than that of MPP^+.

When an illicit drug manufacturer inappropriately heated an intermediate in the synthesis of a retro-ester of meperidine, a so-called designer drug, the 1-methyl-4-phenylpiperidine derivative, dehydrated to give 1-methyl-4-phenyl-1,2,3,6-tetrahydropyridine (MPTP, **1**). It is now well-recognized that MPTP produces a frank Parkinsonian syndrome in man, primates, and certain other animals.[1] This neurotoxin and its metabolites are associated with severe and selective depletion of dopamine in the substantia nigra, a biochemical situation parroted in Parkinson's disease.[2] In attempting to explain the neurotoxic mechanism of MPTP, several hypotheses have been forwarded.[3] The finding that the metabolic end product of MPTP oxidation (i.e., the 1-methyl-4-phenylpyridinium ion MPP^+, **8**) is toxic when applied directly to brain cells indicates that MPTP may serve only as a membrane permeable delivery form for the quaternary salt.[4] On the other hand, studies showing that antioxidants hinder and superoxide ($O_2^{\cdot-}$) dismutase inhibitors exacerbate MPTP effects may indicate that species generated in the conversion of MPTP to MPP^+ mediate toxicity.[5] In either case, the oxidation of MPTP is clearly important for the biochemical manifestations of this material.

Unfortunately, it is difficult to study intermediates in this oxidative process because they are highly energetic and short-lived. Since, therefore, this system is not amenable to simple experimental examination, a theoretical molecular orbital (MO) approach was applied. The MNDO method[6] chosen can provide important information on the stability, structure, mechanism of formation, and reactivity of species that are produced by various pathways. In addition by comparing this conversion to that of other reduced pyridines such as the NADH model, 1-methyl-1,4-dihydronicotinamide, the unique reactivity of MPTP can be better defined and illustrated.

Methods

The calculations were carried out on an IBM 3081 Model K dual processor computer operating at 15 MIPS using the MNDO molecular orbital approximation.[6] The MNDO program was obtained through quantum chemical program exchange (QCPE), converted to VS Fortran, and adapted to run on the IBM 3081 computer. The structural input was generated using the SYBYL/MOPAC interface, and the geometries were found by minimizing the total energy with respect to all structural

Scheme I

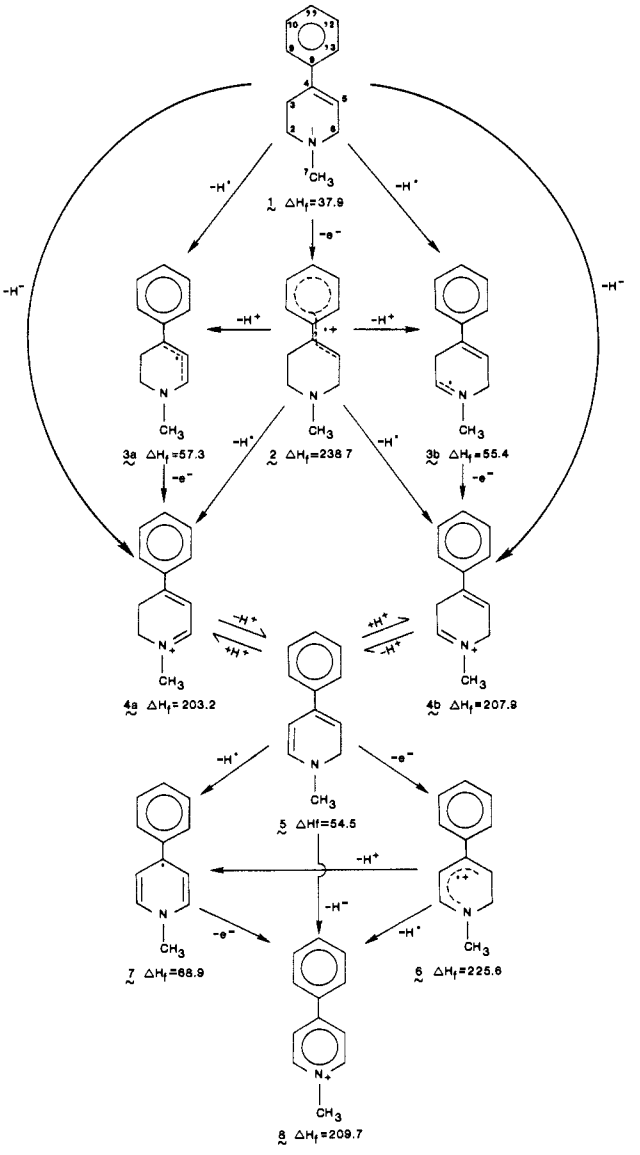

* To whom correspondence should be addressed.

† Part 1 of this series, Correlation Between Hydride Transfer and One-Electron Oxidation of Dihydropyridines and Related Heterocycles: Bodor, N.; Kaminski, J. J. *Theochem.* **1988**, *163*, 315.

‡ Center for Drug Design and Delivery, College of Pharmacy, JHMHC, Box J-497, University of Florida, Gainesville, FL 32610.

§ Pharmatec, Inc., P.O. Box 730, Alachua, FL 32615.

⊥ Schering-Plough Corporation, Pharmaceutical Research Division, Bloomfield, NJ 07003.

0002-7863/88/1510-6337$01.50/0

Table I. Optimized Geometries (Selected Bond Lengths, Bond Angles, and Dihedral Angles) for Various Pyridine Derivatives Generated by the Oxidation of 1-Methyl-4-phenyl-1,2,3,6-tetrahydropyridine (MPTP) by Various Mechanisms[a]

atom no.	1	2	3a	3b	4a	4b	5	6	7	8
					Bond Length (Å)					
1–2	1.456	1.456	1.472	1.393	1.496	1.323	1.404	1.364	1.412	1.388
2–3	1.553	1.553	1.546	1.488	1.539	1.507	1.363	1.421	1.382	1.399
3–4	1.516	1.529	1.491	1.514	1.511	1.513	1.461	1.422	1.423	1.421
4–5	1.354	1.418	1.408	1.346	1.377	1.351	1.357	1.393	1.430	1.419
5–6	1.507	1.505	1.402	1.501	1.440	1.501	1.506	1.503	1.378	1.406
1–6	1.469	1.438	1.392	1.477	1.343	1.507	1.473	1.476	1.414	1.385
1–7	1.460	1.468	1.468	1.467	1.491	1.499	1.462	1.490	1.462	1.498
4–8	1.483	1.432	1.463	1.487	1.478	1.484	1.490	1.484	1.474	1.483
8–9	1.414	1.443	1.422	1.415	1.416	1.415	1.416	1.420	1.422	1.418
9–10	1.405	1.391	1.403	1.405	1.406	1.405	1.406	1.406	1.405	1.405
10–11	1.406	1.417	1.405	1.406	1.407	1.407	1.405	1.407	1.404	1.407
11–12	1.406	1.417	1.405	1.406	1.407	1.407	1.405	1.407	1.404	1.407
12–13	1.405	1.391	1.403	1.405	1.406	1.405	1.406	1.406	1.405	1.405
13–8	1.415	1.448	1.423	1.415	1.419	1.414	1.415	1.424	1.409	1.417
					Bond Angle (deg)					
1–2–3	112.35	112.68	115.36	121.83	114.26	123.72	121.02	120.99	121.09	121.73
2–3–4	110.15	108.68	117.41	115.46	116.71	115.11	120.73	120.51	120.91	118.73
3–4–5	116.76	109.70	118.51	119.91	118.46	119.61	120.28	120.35	117.44	119.40
4–5–6	122.84	122.12	120.35	125.24	121.48	125.61	121.53	120.86	121.28	119.74
7–1–2	117.89	120.28	117.60	117.60	117.05	121.33	120.14	119.92	120.70	120.13
8–4–3	119.51	125.05	119.79	117.50	119.22	117.37	117.97	119.43	120.85	120.32
9–8–4	120.79	122.84	122.08	121.19	121.41	120.39	u20.60	120.34	120.86	120.47
10–9–8	120.68	121.93	121.18	120.88	120.84	120.61	120.56	120.31	120.65	120.47
14–7–1	110.15	111.00	110.11	110.75	109.64	110.87	110.85	110.43	111.19	109.82
					Dihedral Angle (deg)					
1–2–3–4	52.58	55.84	15.68	−6.553	23.96	−0.62	−1.814	−0.849	0	0
2–3–4–5	318.36	302.88	336.28	−4.15	336.69	0.395	−0.177	0.163	0	0
3–4–5–6	1.59	41.97	13.66	1.423	10.86	0.325	0.298	0.177	0	0
7–1–2–6	151.36	189.6	161.33	153.2	180.57	179.96	169.39	174.9	170.35	179.1
8–4–3–5	181.28	187.8	182.85	180.14	183.13	180.03	180.4	191.09	179.6	180.19
9–8–4–3	86.27	7.12	43.06	84.87	59.54	91.73	81.32	63.83	57.5	66.0
10–9–8–4	180.0	180.0	180.0	180.0	180.0	180.0	180.0	180.0	180.0	180.0
14–7–1–2	47.2	30.1	38.68	40.31	41.45	−2.47	37.93	35.19	32.34	29.86

[a] Numbering as in Scheme I.

Table II. Charge Distributions for Various Pyridine Derivatives Involved in the Oxidation of 1-Methyl-4-phenyl-1,2,3,6-tetrahydropyridine (MPTP)[a]

	atomic charges									
atom no.	1	2	3a	3b	4a	4b	5	6	7	8
1	−0.466	−0.487	−0.354	−0.298	−0.271	−0.212	−0.413	−0.276	−0.286	−0.182
2	0.171	0.178	0.167	−0.156	0.135	0.267	0.136	0.198	0.011	0.127
3	0.007	−0.010	0.039	0.102	−0.046	−0.009	−0.189	−0.047	−0.028	−0.079
4	−0.072	−0.022	−0.123	−0.050	0.183	−0.008	0.022	0.035	−0.134	0.155
5	−0.088	0.106	−0.089	−0.100	−0.218	−0.130	−0.145	0.025	−0.029	−0.085
6	0.203	0.172	0.054	0.193	0.313	0.169	0.230	0.137	0.012	0.134
7	0.221	0.223	0.206	0.191	0.169	0.154	0.219	0.174	0.211	0.173
8	−0.039	−0.016	−0.014	−0.044	−0.153	−0.107	−0.042	−0.126	−0.009	−0.150
9	−0.039	0.039	−0.055	−0.038	−0.005	−0.027	−0.039	−0.016	−0.054	−0.012
10	−0.065	−0.081	−0.061	−0.065	−0.056	−0.053	−0.066	−0.054	−0.062	−0.054
11	−0.053	0.110	−0.066	−0.053	0.002	−0.019	−0.055	−0.003	−0.067	−0.003
12	−0.065	−0.073	−0.062	−0.065	−0.057	−0.053	−0.065	−0.052	−0.062	−0.054
13	−0.038	0.012	−0.051	−0.038	−0.007	−0.027	−0.039	−0.018	−0.053	−0.011

[a] Numbering as in Scheme I.

variables using the standard Davidon–Fletcher–Powell optimization procedure.

Results and Discussion

Various oxidative routes for the conversion of MPTP (**1**) to MPP^+ (**8**) are illustrated in Scheme I. Optimized structural

(1) Markey, S. P.; Castagnoli, N.; Trevor, A. J.; Kopin, I. J. *MPTP: A Neurotoxin Producing a Parkinsonian Syndrome*; Academic: Orlando, FL 1986; pp 1–716.

(2) (a) Chiueh, C. C.; Burns, R. S.; Markey, S. P.; Jacobowitz, D. M.; Kopin, I. J. *Life Sci.* **1985**, *36*, 213–218. (b) Burns, R. S.; Chiueh, C. C.; Markey, S. P.; Ebert, M. H.; Jacobowitz, D. M.; Kopin, I. J. *Proc. Natl. Acad. Sci. U.S.A.* **1983**, *80*, 4546–4550. (c) Snyder, S. H.; D'Amato, R. J. *Neurology* **1986**, *36*, 250–258. (d) Jenner, P.; Rupniak, N. M.; Rose, S.; Kelly, E.; Kilpatrick, G.; Lees, A.; Marsden, C. D. *Neurosci. Lett.* **1984**, *50*, 85–90. (e) Mitchell, I. J.; Cross, A. J.; Sambrook, M. A.; Crossman, A. R. *Neurosci. Lett.* **1985**, *61*, 195–200.

(3) Langston, J. W.; Irwin, I. *Clin. Neuropharmacol.* **1986**, *9*, 485–507.

(4) (a) Markey, S. P.; Johannessen, J. N.; Chiueh, C. C.; Burns, R. S.; Henkenham, M. A. *Nature (London)* **1984**, *311*, 464–467. (b) Langston, J. W.; Irwin, I.; Langston, E. B.; Forno, L. S. *Neurosci. Lett.* **1984**, *48*, 87–92. (c) Irwin, I.; Langston, J. W. *Life Sci.* **1985**, *36*, 207–212. (d) Tadano, T.; Satoh, N.; Sakuma, I.; Matsumura, T.; Kisara, K.; Arai, Y.; Kinemuchi, H. *Life Sci.* **1987**, *40*, 309–318.

(5) (a) Perry, T. L.; Yong, V. W.; Clavier, R. M.; Jones, K.; Wright, J. M.; Foulks, J. G.; Wall, R. A. *Neurosci. Lett.* **1985**, *60*, 109–114. (b) Sershen, H.; Reith, M.; Hashim, A.; Lajtha, A. *Neuropharmacol.* **1985**, *24*, 1257–1259. (c) Corsini, G. V.; Pintus, S.; Chiueh, C. C.; Weiss, J. F.; Kopin, I. J. *Eur. J. Pharmacol.* **1985**, *119*, 127–128.

(6) Dewar, M. J. S.; Thiel, W. *J. Am. Chem. Soc.* **1977**, *99*, 4899–4907.

information is given in Table I and charge distributions in Table II. Certain structures were not considered in this study such as the intermediates described below.

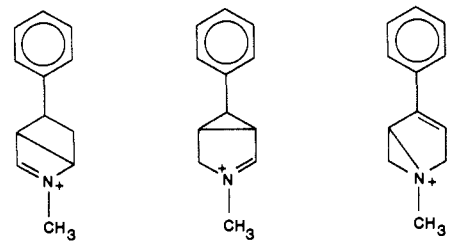

These were excluded since previous examination of similar bicyclic pyridine species showed that they were energetically unlikely.[7]

MPTP (**1**) is a relatively stable molecule in which the phenyl group is oriented approximately 85° (ϕ9–8–4–3) out of the plane of the tetrahydropyridine ring.[8] This reduces steric interaction that can occur between hydrogens located on C-3 and C-9 (see numbering in Scheme I) and/or C-5 and C-13. The highest occupied molecular orbital (HOMO) is of the σ-type and is low in energy (–9.30 eV). The enzyme thought to be responsible for initiating the conversion of **1** to **8** is monoamine oxidase B (MAO-B), a conclusion based on the effect of various inhibitors of MAO-B as well as by studies with the purified enzyme.[11] In addition, it is known that catalysis of the oxidation of **1** results in suicide inactivation of MAO-B.[12] MAO-B is thought to oxidize substituted amines by an initial electron removal.[13] If this occurs in the case of **1**, the radical cation **2** is produced. The energy required to effect this one-electron oxidation is high (>200 kcal/mol) and the species generated is exceedingly unstable. This instability is associated with the destruction of the aromatic character of the pendant 4-phenyl group as indicated by the perturbed geometry and charge distribution. The associated planarization [(ϕ9–8–4–3) changes from 86.3° in **1** to 7.1° in **2**] also increases steric interactions as hydrogens attached to C-3 and C-9 come within less than 2 Å of each other. There appears to be little involvement of the N-1 in the HOMO. This unstable radical cation can subsequently deprotonate giving either **3a** or **3b** or can lose atomic hydrogen to give **4a** or **4b**. In radical **3a**, which results from proton loss from C-6, the free radical electron is delocalized over C-4 and C-6 as indicated by the large atomic orbital (AO) coefficient contributions to the HOMO. In addition, as shown in Table I, the C-4–C-5 and C-5–C-6 bonds are essentially equivalent. The charge is most concentrated on C-4 of the allylic radical. In this species as in all subsequent ones, the phenyl ring is again oriented out of the plane of the incipient pyridine ring. Removal of a proton from C-2 of **2** gives **3b**. In this structure the free radical electron is shared by N-1 and C-2 and in general this intermediate is more product-like than the isomeric radical (i.e., more like **4b** than **3a** is like **4a**). One-electron oxidation of **3a** or **3b** yields the corresponding dihydropyridinium salts **4a** and **4b** as does removal of atomic hydrogen from C-6 or C-2 from **2**, respectively. Compound **4a** ($MPDP^+$) has been detected chromatographically in various enzymatic preparations after treatment with **1**.[1] On the basis of this study and regardless of the path taken (i.e., Law of Hess), it is clear that **4a** predominates over **4b** since the former is 4.7 kcal/mol more stable than the latter. The indicated equilibrium (Scheme I) between **4a** and **4b** via **5** is known to occur in vitro since treatment of **4a** with nucleophiles such as cyanide gives rise to both the 5- and 2-substituted tetrahydropyridines.[14] Interestingly, the charge densities calculated for **4a** and **4b** accurately predict these reactions. The 2,3-dihydropyridinium ion **4a** is also suspected as a toxic intermediate since the electrophile could react with cellular constituents to produce alkylated macromolecules. This does not appear to be the case since adducts of **4a** and amino acids do not form. In addition, a stable analogue of **4a** (i.e., the 3,3-dimethyl derivative) was found to be much less toxic than **8** when administered directly to neurons.[15]

The subsequent reactions of **4a** have again been the subject of controversy and both enzymatic and nonenzymatic routes have been proposed.[3] Early in its study, it was found that at high concentrations **4a** would disproportionate to yield **8** and **1**.[1] The mechanism for this reaction, which has also been envoked in vivo from time to time, was proposed by Castagnoli and is described below:[13]

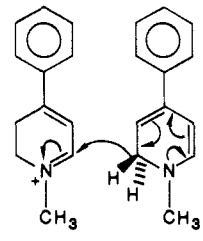

In this representation, a hydride from C-6 is transferred to C-5 of **4a**. This is consistent with the assigned charge distributions generated in Table II. The conversion of **4a** to **8** has also been shown to be catalyzed by MAO-B, denatured enzyme, and other materials such as metal chelates.[1,17,18] The π-type HOMO of **5** (–8.07 eV) is more energetic than that associated with **1** by 1.23 eV. This different is evident in comparing the corresponding one-electron oxidations which is approximately 30 kcal/mol more exergonic in the case of **5**. The resulting radical cation **6** is stabilized by delocalization of the charge and spin over the dihydropyridine π-network. Loss of a proton yields the pyridinyl radical **7**. As illustrated in eq 1, which represents the π-type HOMO for this molecule, the free radical electron is localized on C-4. This is consistent with the behavior of various stable pyridinyl radicals.[19]

$$\Psi^7_{HOMO} = 0.407(\text{N-1}p_z) - 0.431(\text{C-2}p_z) - 0.130(\text{C-3}p_z) + 0.600(\text{C-4}p_z) - 0.132(\text{C-5}p_z) - 0.419(\text{C-6}p_z) \quad (1)$$

In addition, the geometry generated for this species reflects the 1,4-dihydropyridine structure. One-electron oxidation of this

(7) Bodor, N.; Pearlman, R. *J. Am. Chem. Soc.* **1978**, *100*, 4946–4953.

(8) While structural information is limited on MPTP (1), the X-ray crystal structure for the hydrochloride salt of MPTP has been elucidated. A comparison of the configuration determined by this technique to that generated by MNDO is in good agreement. The C2–C3 bonds are within 0.025 Å, the C4═C5 within 0.03 Å, and the bond separating the two ring systems (C4–C8) within 0.022 Å. Bond angles are also within experimental error. The main difference in the theoretically and experimentally determined structure is the orientation of the phenyl group. X-ray data indicate it is within 7° of the tetrahydropyridine[9] ring while MNDO calculations suggest it is approximately 53° out of the plane. Differences of this type are not uncommon when structurally unhindered molecules such as those in the gas phase (or structures generated theoretically) are compared to molecules in crystalline matrices. The X-ray crystal structure for biphenyl, for example, was found to be within 10° of planarity while MNDO and gas-phase studies suggested torsion angles of 63° and 42°, respectively.[10]

(9) Klein, C.; Borne, R.; Stevens, E. *Pharm. Res.* **1985**, *2*, 192–194.

(10) Busing, W. *Acta Cryst.* **1983**, *A39*, 340–347.

(11) (a) Chiba, K.; Trevor, A.; Castagnoli, N. *Biochem. Biophys. Res. Commun.* **1984**, *120*, 574–578. (b) Heikkila, R.; Manzino, L.; Cabbat, F. S.; Duvoisin, R. C. *J. Neurochem.* **1985**, *45*, 1049–1054.

(12) (a) Salach, J. I.; Singer, T. P.; Castagnoli, N.; Trevor, A. *Biochem. Biophys. Res. Commun.* **1984**, *125*, 831–835. (b) Singer, T. P.; Salach, J. I.; Crabtree, D. *Biochem. Biophys. Res. Commun.* **1985**, *127*, 707–712.

(13) Silverman, R. B.; Yamasaki, R. B. *Biochemistry* **1984**, *23*, 1322–1332.

(14) (a) Baker, J. K.; Borne, R. F.; Davis, W. M.; Waters, I. W. *Biochem. Biophys. Res. Commun.* **1984**, *125*, 484–490. (b) Gessner, W.; Brossi, A.; Shen, R.; Abell, C. W. *FEBS Lett.* **1985**, *183*, 345–348.

(15) Sayre, L. M.; Arora, P. K.; Feke, S. C.; Urback, F. L. *J. Am. Chem. Soc.* **1986**, *108*, 2464–2466.

(16) Peterson, L. A.; Caldera, P. S.; Trevor, A.; Chiba, K.; Castagnoli, N. *J. Med. Chem.* **1985**, *28*, 1432–1436.

(17) Castagnoli, N.; Chiba, K.; Trevor, A. J. *Life Sci.* **1985**, *36*, 225–230.

(18) (a) Korytowski, W.; Felix, C. C.; Kalyanaraman, B. *Biochem. Biophys. Res. Commun.* **1987**, *147*, 354–360. (b) Korytowski, W.; Felix, C. C.; Kalyanaraman, B. *Biochem. Biophys. Res. Commun.* **1987**, *144*, 692–698.

(19) Pryor, W. A. *Free Radicals in Biology*; Academic: New York, 1976; Vol. II, pp 1–53.

Scheme II

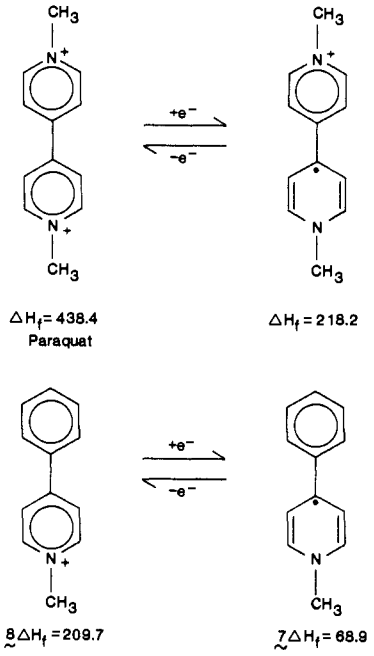

radical gives the aromatic pyridinium salt **8**.

Reactive Intermediates. Several of the radicals depicted in Scheme I could react with oxygen to generate cytotoxic superoxide ($O_2^{\bullet-}$) and hydrogen peroxide.[19] Radicals such as **3a** or **7** are prime candidates to enter into such reactions. For example, it has been shown that **7** can be generated either by Fe(III) oxidation of **4a**[18] or one-electron reduction of **8**[20] and that this radical reacts with O_2 presumably giving rise to $O_2^{\bullet-}$. These studies suggest that **7** is a relatively stable radical, consistent with the present data. The circumstance for **3a** is more problematic. This material has been generated by various techniques[20] or suspected as an intermediate,[21] but controversy surrounds whether it is involved in the oxidation of **1**. Recently, pulse radiolysis and laser flash photolysis studies showed that **3a** does not react to give **4a** and the authors conclude that it is not involved in vivo in the conversion of **1** to **4a**.[20] In addition, various reports have represented **4a** and **7** as radicals that are stabilized by phenyl ring involvement. This assumption is not supported by this present study.[20,21]

The possible involvement of **8** in redox cycling has also been suggested.[3] In this process a pyridinium salt undergoes one-electron reduction to yield the pyridinyl radical. This species then reacts with O_2 to form $O_2^{\bullet-}$ and the quaternary ion is regenerated only to enter the cycle again. This mechanism is thought to play a prominent role in pulmonary toxicity of the herbicide paraquat.[3] In order for this to occur in the case of **8**, the one-electron reduction of **8** should be facile. Calculations suggest, however, that the process is substantially more endergonic in the case of **8** (Scheme II), consistent with the published half-wave potentials for **8** (E_0 = −1.18 V) and for paraquat (E_0 = −0.44 V).[4,15] It was also suggested that **4a** may participate in this cycle.[15] The one-electron reduction of **4a** is, in fact, 6 kcal/mol more favorable than that for **8**, but the lability of **4a** in tissue and the questioned role of **3a** makes this possibility remote.

NADH Model Studies. While the oxidation of **1** is associated with cellular destruction, the oxidation of other reduced pyridines is necessary for continued cellular functioning. In this category is the coenzyme nicotinamide adenine dinucleotide (NADH), which acts as an electron transport couple in cellular respiration.[22] In addition, 1,4-dihydronicotinamides and -nicotinates are used

Scheme III

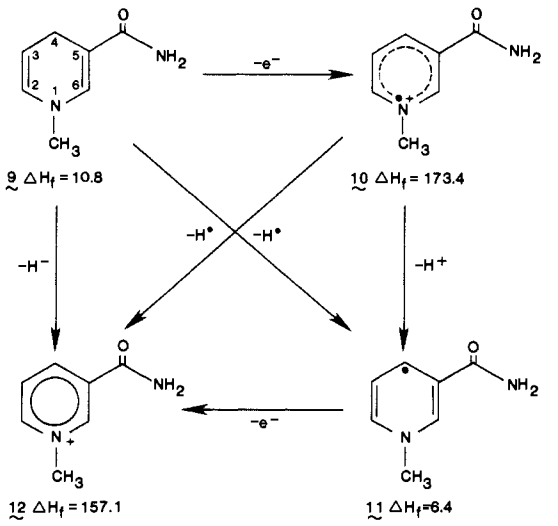

as molecular carriers to target drugs to the brain.[23] Neither of these processes is associated with any MPTP effects.[24] Therefore, the oxidation of an NADH model was examined. The mechanism of oxidation of 1-substituted 1,4-dihydronicotinamides is not certain and concerted hydride transfer[25] and sequential electron, hydrogen atom[26] or electron, proton, electron[26] processes have been proposed depending on reaction conditions. These routes were examined (Scheme III). The model dihydropyridine, 1-methyl-1,4-dihydronicotinamie (**9**), has a π-type HOMO that is intermediate in energy between **1** and **5** (i.e., −8.51 eV). Hence, **9** is more easily oxidized than **1** and the intermediates produced are of much lower energy. Also **9** is more stable than 1,2-dihydropyridine (**5**). This results from extended conjugation associated with the amide function. Other stabilizing factors can be demonstrated by examining the HOMO's for the two compounds (eq 2 and 3). As illustrated by eq 2 and 3, the contributions by the sp^3 carbon (C-4 in **9** and C-6 in **5**) are greater in the case of **9**, indicating greater homoaromaticity. Both compounds appear to be stabilized by contributions of hydrogens attached to the sp^3 carbon (i.e., hyperconjugation) although the effect is slightly larger in the case of **9**.[7] Loss of an electron from **9** generates the radical cation **10**. This species unlike **2** is stabilized by spin and charge delocalization over the π-network. The loss of a proton from **10** gives the radical **11**. In this radical, the radical electron is localized on the central carbon (C-4) of the dienamine consistent with published reports.[16] One-electron oxidation of this material gives the pyridinium salt **12**. Calculations suggest that the one-electron reduction of **12** is approximately 10 kcal/mol more exergonic than the corresponding reduction of **8**. This result is consistent with experimentally derived half-wave potentials for **12** (E_0 = −0.85 V) and for **8** (−1.18 V).[15,27c]

$$\Psi^9_{HOMO} = 0.530(N\text{-}1p_z) - 0.213(C\text{-}2p_z) - 0.502(c\text{-}3p_z) + 0.107(C\text{-}4p_z) - 0.478(C\text{-}5p_z) - 0.269(C\text{-}6p_z) - 0.195(H(\text{on C-4})) + 0.193(H(\text{on C-4})) \quad (2)$$

$$\Psi^5_{HOMO} = 0.474(N\text{-}1p_z) - 0.368(C\text{-}2p_z) - 0.537(C\text{-}3p_z) + 0.233(C\text{-}4p_z) + 0.446(C\text{-}5p_z) - 0.067(C\text{-}6p_z) - 0.187(H(\text{on C-6})) + 0.182(H(\text{on C-6})) \quad (3)$$

(20) Chacon, J. N.; Chedekel, M. R.; Land, E. J.; Truscott, T. G. *Biochem. Biophys. Res. Commun.* **1987**, *144*, 957–964.
(21) Poirier, J.; Donaldson, J.; Barbeau, A. *Biochem. Biophys. Res. Commun.* **1985**, *128*, 25–33.
(22) Everse, K.; Anderson, B. M.; You, K. *The Pyridine Nucleotide Coenzymes*; Academic: New York, 1982.
(23) (a) Bodor, N.; Farag, H.; Brewster, M. *Science (Washington, D.C.)* **1981**, *214*, 1370–1372. (b) Bodor, N.; Brewster, M. *Pharmacol. Ther.* **1983**, *19*, 337–386. (c) Brewster, M.; Estes, K.; Bodor, N. *J. Med. Chem.* **1988**, *31*, 244–249.
(24) Brewster, M. E.; Estes, K. S.; Perchalski, R.; Bodor, N. *Neurosci. Lett.*, in press.
(25) (a) Powell, M. F.; Bruice, T. C. *J. Am. Chem. Soc.* **1983**, *105*, 1014–1021. (b) Powell, M. F.; Bruice, T. C. *J. Am. Chem. Soc.* **1983**, *105*, 7139–7149.
(26) Bunting, J. W.; Chew, V. W.; Chu, G.; Fitzgerald, N. P.; Gunasekara, A.; Oh, H. T. *Bioorg. Chem.* **1984**, *12*, 141–157.

In conclusion, optimized geometries, charge distributions, and molecular orbital structure were generated for MPTP and intermediates in its conversion to MPP^+. Sequential electron, proton, electron mechanisms as well as electron, hydrogen atom and concerted hydride transfer were considered. The data show the initial ionization of MPTP is highly energonic and results in the formation of intermediates capable of interacting with O_2 to generate $O_2^{\bullet-}$ and possibly causing enzymatic inactivation or neurotoxocity. The large resonance energy of MPP^+ was demonstrated as well as the potent reducing potential of $MPP^\bullet$. In addition, the reaction of MPTP was shown to be both quantitatively and qualitatively different from the oxidation of an NADH analogue.

(27) (a) Ohno, A.; Shio, T.; Yamamoto, H.; Oka, S. *J. Am. Chem. Soc.* **1981**, *103*, 2045–2048. (b) Carlson, B. W.; Miller, L. L.; Neta, P.; Grodkowski, J. *J. Am. Chem. Soc.* **1984**, *106*, 7233–7239. (c) Powell, M. F.; Wu, J. C.; Bruice, T. C. *J. Am. Chem. Soc.* **1984**, *106*, 3850–3856.

Acknowledgment. The authors would like to thank Ms. Anna Marie Martin for her help in preparing this manuscript. This work was supported in part by a grant from the NIH (GM 27167).

Resonance Raman Studies of Myoglobin Single Crystals

Dimitrios Morikis, J. Timothy Sage, Apostolos K. Rizos,† and Paul M. Champion*

Contribution from the Department of Physics, Northeastern University, Boston, Massachusetts 02115. *Received November 2, 1987*

Abstract: We investigate the resonance Raman scattering of myoglobin (Mb) single crystals in order to probe the similarities and/or differences between solution and crystal structures of biological molecules. Resonant light scattering spectroscopy provides a high-resolution map of the vibrational frequencies associated with the protein active site and can be applied to solution, crystalline, or frozen states of the sample. We find that the metmyoglobin samples have active site heme structures that are nearly independent of the sample state. However, when the carbon monoxide adduct is formed, the MbCO crystal spectrum reveals two distinct modes of CO binding, compared to a single Raman mode in the solution structure. Unusual observations involving the photoreduction of metMb and the photolysis of MbCO in the crystalline state are also reported. A preliminary polarization analysis of the Raman scattering from Mb crystals is also presented.

We present resonance Raman spectra of single crystals of myoglobin (Mb) and compare them to solution spectra. With some key exceptions, the relative Raman intensities and frequencies of the crystals are found to be nearly identical with the solution samples. The polarization of the Raman scattering is also analyzed and the depolarization ratios ($\rho = I_\perp/I_\parallel$) of the heme vibrations in metMb are found to vary strongly with the crystal orientation. An increase of the laser flux at the metMb crystal leads to a photoreduction process that produces a species whose Raman spectrum is nearly identical with that of deoxymyoglobin. Carbon monoxide bound myoglobin crystals (MbCO) are also examined. We find two different types of CO binding in the room temperature crystal as evidenced by their distinct Fe–CO vibrational frequencies at 491 and 508 cm^{-1}. Surprisingly, we are unable to completely photodissociate the MbCO crystals in order to examine the deoxy photoproduct. This suggests that the CO is trapped in the distal pocket of the MbCO crystal at room temperature and that the geminate rebinding rates are rapid compared to the laser-driven photolysis.

The Raman spectra are collected with use of continuous wave laser excitation wavelengths in the region λ_{ex} = 415–430 nm, which is resonant with the Soret band of heme proteins. The detection of the scattered radiation is accomplished with use of an intensified diode array detector and a triple grating spectrograph. The crystals are grown according to the method of Kendrew and Parrish[1] with use of sperm whale metMb obtained commercially. The crystallographic coordinates of Takano are used to obtain the heme orientations.[2]

Figure 1 displays the high-frequency (950–1700 cm^{-1}) and the low-frequency (200–950 cm^{-1}) Raman spectra of metMb under three different conditions (crystal high-flux, crystal low-flux, and solution). The high laser flux condition (ca. 30 W/cm^2) leads to an apparent photoreduction of the metMb crystal (a). This is evidenced by the shift of the oxidation state marker band[3] (ν_4) from 1372 to 1355 cm^{-1} as well as by the appearance of the iron–histidine axial ligand mode ($\nu_{Fe\text{-}His}$) at 219 cm^{-1}.

Upon detailed comparison of the crystal and solution Raman spectra (b and c), we find no reproducible frequency differences between the two species. This provides the first direct, high-resolution, spectroscopic evidence that the active site heme structure is unperturbed upon crystallization. The favorable comparison between crystal and solution structures is reminiscent of early cryogenic resonance Raman studies of heme proteins[4] where it was shown that the heme structure was not detectably modified upon freezing the solution. It seems that the interaction of the globular protein material and the heme group is remarkably stable to perturbations induced by phase change.

In Figure 2 we display resonance Raman spectra of MbCO crystals, formed using the method described by Kuriyan et al.[5] The Fe–CO stretching mode found[6] near 500 cm^{-1} is of particular interest, since the presence of two vibrational frequencies at 508 and 491 cm^{-1} is clearly visible in the crystal data (trace b). The solution spectra are dominated by the presence of a single mode at 508 cm^{-1} (trace c). This implies that the relative populations of distal pocket structures, responsible for the orientation and/or polarization of the Fe–CO moiety, are different in crystalline material than in solution at pH 7. The observation of multiple

†Present address: Department of Chemistry, University of Crete, 711 10 Iraklion, Greece.

(1) Kendrew, J. C.; Parrish, R. G. *Proc. R. Soc. London A* **1956**, *238*, 305–324.
(2) Takano, T. *J. Mol. Biol.* **1977**, *110*, 537–568.
(3) Spiro, T. G. In *Iron Porphyrins*, Part II; Lever, A., Gray, H., Eds.; Addison-Wesley: Reading, MA, 1983.
(4) Champion, P. M.; Collins, D. W.; Fitchen, D. B. *J. Am. Chem. Soc.* **1976**, *98*, 7114–7115.
(5) Kuriyan, J.; Wilz, S.; Karplus, M.; Petsko, G. *J. Mol. Biol.* **1986**, *192*, 133–154.
(6) Tsubaki, M.; Srivastava, R.; Yu, N. T. *Biochemistry* **1982**, *21*, 1132–1140.

0002-7863/88/1510-6341$01.50/0